Solid-State ^{13}C CPMAS NMR and Molecular Mechanics Study of Conformational Recognition in Mixed Crystals of Two Phenylalkyl Ketones

M. A. Garcia-Garibay,* Steve H. Shin, I. Chao,† K. N. Houk, and S. I. Khan

Department of Chemistry and Biochemistry, University of California, Los Angeles, California 90024

Received December 21, 1993. Revised Manuscript Received March 4, 1994®

A detailed structural analysis of a dilute mixed crystal of ^{13}C-Me-labeled 1,2-diphenylpropanone (1) in 2-methyl-1,2-diphenylpropanone (2) has been carried out with the help solid state ^{13}C cross polarization and magic angle spinning (CPMAS) NMR, molecular mechanics calculations of mixed crystal models, and X-ray diffraction techniques. After characterization of the crystal phases of the pure components, mixed crystals prepared with 1–5% 1 (99.9% ^{13}C-Me labeled) were investigated by solid-state NMR with the goal of addressing structural questions at the molecular level. In the mixed crystals, the NMR signals assigned to the host remained unperturbed, while signals of 1 were different from those observed in its pure crystal phases (racemic and enantiomorphous). Two different types of spectra were observed from samples obtained in different mixed crystallization experiments. We postulate that two groups of signals in one type arise from disorder of the guest in the crystal host when guest molecules crystallize in their two lowest energy conformers. In contrast, ordered mixed crystallization in the second type results in one signal assigned to the guest in its lowest energy conformer. These conclusions are supported by molecular mechanics calculations carried out for gas phase and model crystal systems.

Introduction

Organic mixed crystals or solid solutions are multicomponent solid systems with variable composition and with the crystal structure of one of the components.[1,2] The use of mixed crystals in solid-state organic chemistry[3] offers the possibility for controlling the concentration of prospective reactants, for carrying out competition experiments, (sensitization, quenching, scavenging) for inducing changes in crystal symmetry,[4] and for the incorporation of noncrystalline guests into suitable crystalline environments. The importance of mixed crystallization in molecular recognition phenomena has also been recently recognized.[5,6]

Important applications of solid state chemistry come from the elucidation of structure–reactivity correlations where the distance and orientation between prospective reactants and their reaction trajectories may be deduced from accurate X-ray structural data.[3,7] While structure–reactivity correlations involving a reactive guest may have important applications in this area, examples involving the use of mixed crystals commonly assume the structure of the guest from the crystal structure of the host.[8] Experimental strategies to obtain structural information

* To whom correspondence should be addressed.
† Current address: Institute of Chemistry, Academia Sinica, Taipei, Taiwan.

® Abstract published in *Advance ACS Abstracts*, August 15, 1994.

(1) Kitaigorodskii, A. I. *Mixed Crystals*; Springer-Verlag: Berlin, 1984.

(2) Mixed crystals differ from solid-state complexes in that the latter have defined stoichiometries and crystal structures distinct from those of the pure components. Complexes may form through hydrogen bonding: (a) Etter, M. C.; Huang, K. S. *Chem. Materials* **1992**, *4824*. (b) Görbitz, C. H.; Etter, M. C. *J. Am. Chem. Soc.* **1992**, *114*, 627. (c) Etter, M. C.; Reutzel, S. M.; Choo, C. G. *J. Am. Chem. Soc.* **1993**, *115*, 4411. (d) Garcia-Tellado, F.; Geib, S. J.; Goswami, S.; Hamilton, A. D. *J. Am. Chem. Soc.* **1991**, *113*, 9265. (e) Yang, J.; Fan, E. K.; Geib, S. J.; Hamilton, A. D. *J. Am. Chem. Soc.* **1993**, *115*, 5314. (f) Dvorak, D.; Zavada, J.; Etter, M. C.; Loehlin, J. H. *J. Org. Chem.* **1992**, *57*, 4839. Through charge-transfer interactions: (a) Prout, C. K.; Kamenar, B. In *Molecular Complexes*; Foster, R., Ed.; Elek Science: London, 1973; p 151. (b) Foster, R. *Organic Charge-Transfer Complexes*; Academic Press: London, 1969; p 216. Complexes may also form by inclusion of the guest in the hydrophobic cavities of suitable hosts: (a) Saenger, W. *Angew. Chem., Int. Ed. Engl.* **1980**, *19*, 344. (b) Tabushi, I.; Kuroda, Y. *Adv. Catal.* **1983**, *32*, 417. (c) Usha, M. G.; Wittebort, R. J. *J. Am. Chem. Soc.* **1992**, *114*, 1541. (d) Bender, M. L.; Komiyama, M. *Cyclodextrin Chemistry*; Springer-Verlag: New York, 1977.

(3) (a) Gabarskczyk, J. B.; Jones, D. W., Eds. *Organic Crystal Chemistry*; Oxford: Cambridge, 1991. (b) Desiraju, G. R. *Organic Solid State Chemistry*; Elsevier: Amsterdam, 1987. (c) Ramamurthy, V.; Venkatesan, K. *Chem. Rev.* **1987**, *87*, 433–81. (d) Scheffer, J. R.; Garcia-Garibay, M.; Nalamasu, O. In *Organic Photochemistry*; Padwa, A., Ed.; Marcel Dekker, Inc.: New York, 1987; Vol. 8; p 249.

(4) (a) Vaida, M.; Shimon, L. J. W.; van Mil, J.; Ernst-Cabrera, K.; Addadi, L.; Leiserowitz, L.; Lahav, M. *J. Am. Chem. Soc.* **1989**, *111*, 1029. (b) Vaida, M.; Popovitz-Biro, R.; Leiserowitz, L.; Lahav, M. In *Photochemistry in Organized and Contrained Media*; Ramamurthy, V., Ed.; VCH, New York, 1991; pp 247–302.

(5) (a) McBride, J. M.; Bertman, S. B. *Angew. Chem.* **1989**, *101*, 342. (b) McBride, J. M.; Bertman, S. B.; Cioffi, D. Z.; Segmuller, B. E.; Weber, B. A. *Mol. Cryst. Liq. Cryst.* **1988**, *161 (Pt. B)*, 1. (b) Searle, M. S.; Williams, D. H. *J. Am. Chem. Soc.* **1992**, *114*, 10690. (c) Kahr, B.; McBride, J. M. *Angew. Chem., Int. Ed. Engl.* **1992**, *31*, 1. (d) Gopalan, P.; Peterson, N. L.; Crundwell, G.; Kahr, B. *J. Am. Chem. Soc.* **1993**, *115*, 3366.

(6) Vaida, M.; Shimon, L. J. W.; Weisinger-Lewin, Y.; Frolow, F.; Lahav, M.; Leiserowitz, L.; McMullan, R. K. *Science* **1988**, *241*, 1475.

(7) (a) Schmidt, G. M. J. In *Reactivity of the Photoexcited Organic Molecule*; John Wiley & Sons: London, 1967; pp 227–288. (b) Schmidt, G. J. M. *Pure Appl. Chem.* **1971**, *27*, 647. (c) Schmidt, J. M. J. *Solid State Photochemistry*; Ginsburg, D., Ed.; Verlag Chmie: New York, 1976. (d) Scheffer, J. R. In *Solid State Organic Chemistry*; Desiraju, G. R., Ed.; VCH: Amsterdam, 1987; pp 1–45. (e) Scheffer, J. R.; Pokkuluri, P. R. In *Photochemistry in Organized and Contrained Media*; Ramamurthy, V., Ed.; VCH, New York, 1991; pp 185–246. (f) Scheffer, J. R.; Dzakpasu, A. A. *J. Am. Chem. Soc.* **1978**, *100*, 2163.

(8) For a few examples see: (a) Chi, K.-M.; Calabrese, J. C.; Miller, J. S. *Mol. Cryst. Liq. Cryst.* **1989**, *176*, 185. (b) Hasegawa, M.; Kinbara, K.; Adegawa, Y.; Saigo, K. *J. Am. Chem. Soc.* **1993**, *115*, 3820. (c) Hochstrasser, R. M. *J. Chem. Phys.* **1964**, *40*, 1038. (d) Hoshi, N.; Hara, K.; Yamauchi, S.; Hirota, N. *J. Phys. Chem.* **1991**, *95*, 2146. (e) Buntkowsky, G.; Nack, M.; Stehlik, D.; Vieth, H. M. *Isr. J. Chem.* **1989**, *29*, 109. (f) Griffin, G. W.; O'Connel, E. J.; Kelliher, J. M. *Proc. Chem. Soc.* **1964**, 337. (g) Garcia-Garibay, M.; Scheffer, J. R.; Trotter, J.; Wireko, F. *Tetrahedron Lett.* **1987**, *28*, 1741.

0897-4756/94/2806-1297$04.50/0

Chart 1

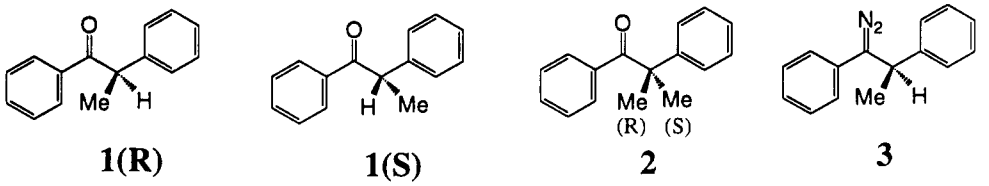

1(R) 1(S) 2 3

Chart 2

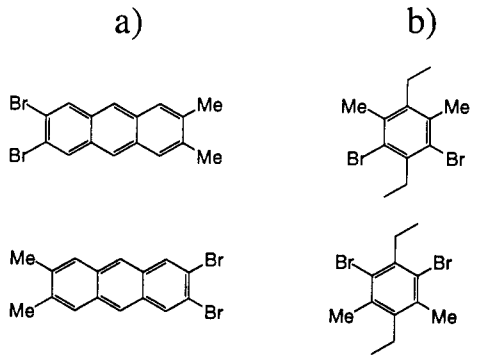

of diluted mixed crystals are therefore highly desirable, and with this in mind we have explored the use of solid-state CPMAS NMR on the structural characterization of mixed crystals between two closely related compounds: 1,2-diphenylpropanone (1) and 2-methyl-1,2-diphenylpropanone (2, Chart 1).

The choice of ketones 1 and 2 for this study comes partially from their use as a model for mixed crystals involving analogous photoreactive diazo compounds such as 1,2-diphenyl-diazopropane (3) currently studied in our laboratory.[9] Our expectation that compounds 1 and 2 should display solid-state solubility follows from their structural similarity and from the lack of strong packing perturbations such as those involved when hydrogen bonding and ionic interactions are present.[1] Also of interest is the possibility that ketones 1 and 2 may display mixed crystallization with positional disorder such as that observed in compounds with nonidentical substituents occupying a given crystallographic position such as the two examples in Chart 2.

In analogy with the compounds in Chart 2 where bromine and methyl groups occupy the same crystallographic positions,[10,11] crystals of ketones 1 and 2 may display positional disorder involving the hydrogen and methyl groups at the α-carbon in the guest. This requires the two enantiotopic methyl groups in ketone 2 (labeled *R* and *S* in Chart 1) to be replaced by the methyl group of either enantiomer of ketone 1 (e.g., **1R** and/or **1S**). In contrast to the examples of Chart 2 where a rigid-body rotation may suffice for substitutional replacement, the substitution of methyl and hydrogen groups in ketones 1 and 2 may involve two different conformations (*vide infra*). Another significant difference from an experimental point of view is that substitution in the examples of Chart 2 involves a heavy bromine atom with high X-ray scattering power. The detection of positional disorder in dilute mixed crystals (1–5%) involving only hydrogen and carbon should be very difficult by X-ray diffraction techniques. Nonetheless, the expected crystallographic and magnetic nonequivalency of the two methyl groups suggests a simple experimental strategy based on the ^{13}C labeling of the methyl group of 1 and on the use of high resolution CPMAS NMR.[12] The ^{13}C label should act as a useful structural probe insofar as the chemical shift of the methyl group is determined by its magnetic environment in the crystal. The label also ensures easy detection of the guest with incorporation levels as low as 1% that are well under the values required for X-ray crystallographic analysis.[10] Finally, to complement our analysis, we have carried out computational studies to gain insight into the conformational properties of ketones 1 and 2 both in the gas phase and in the crystal. This information has been analyzed with X-ray diffraction data of the host as well as through the spectral characterization of mixed crystalline samples.

Experimental Section

Racemic samples of 1,2-diphenylpropanone 1 and of 1,2-diphenyl-2-methyl-1-propanone were obtained from the enolate of 1,2-diphenylethanone (Aldrich) prepared in anhydrous ether or *t*-BuOH with KH or KO-*t*-Bu, respectively, followed by addition of MeI according to known procedures.[13] Samples of ^{13}C-Me-labeled 1 were obtained in a similar fashion using [^{13}C]-MeI (Aldrich 99.9% ^{13}C). Optically enriched (*S*)-(+)-1,2-diphenylpropanone was prepared from the ethyl ester of (*L*)-alanine hydrochloride by the procedure of McKenzie et al.[14]

Crystallizations were carried out from various solvents and from the melt with 200–300 mg of pure components or with mixtures of known composition. Crystallizations from solution were carried out by slow evaporation and to dryness. No differences in composition between the liquid and solid phases were observed within our analytical error limits with guest concentration up to ca. 2–3%. All of the labeled mixed crystals were prepared with [^{13}C]methyl-1,2-diphenylpropanone originating from the same preparation. Several large crystals (5–20 mg) were cut, and the composition of the pieces was separately analyzed by GLC in a search for an inhomogeneous deposition of the guest. Also analyzed were smaller crystals randomly picked from polycrystalline specimens. No significant differences in composition could be found between different crystal pieces or between different crystals from a given batch.

Solution ^1H and ^{13}C NMR spectra were recorded in a Bruker spectrometer at 360 MHz in $CDCl_3$ with TMS as internal standard. Solid-state spectra with cross polarization and magic angle spinning (CPMAS) were recorded in a Bruker MSL 300 instrument at 300 MHz in 7-mm sapphire rotors. For solid state spectra, ^1H decoupling fields of ca. $\gamma B_1/2\pi$ = 40 kHz were employed with carefully matched Hartman–Hahn condition and a critical adjustment of the magic angle. The Me signal of external

(9) Garcia-Garibay, M. A.; Shin, S. H.; Jernelius, J., unpublished results.
(10) (a) Jones, R. D. G.; Welberry, T. R. *Acta Crystallogr.* **1981**, *B37*, 1125. (b) Jones, R. D. G.; Welberry, T. R. *Acta Crystallogr.* **1980**, *B36*, 852.
(11) Gavezzotti, A.; Simonetta, M. In *Organic Solid State Chemistry*; Desiraju, G., Ed.; Elsevier: Amsterdam, 1987; p 391.
(12) For previous studies employing solid-state NMR in the study of mixed crystalline systems see: (a) Cheng, J. L.; Xenopoulos, A.; Wunderlich, B. *Mol. Cryst. Liq. Cryst.* **1993**, *225*, 337. (b) Cheng, J. L.; Xenopoulos, A.; Wunderlich, B. *Mol. Cryst. Liq. Cryst.* **1992**, *220*, 105. (c) White, M. A.; Wasylishen, R. E.; Eaton, P. E.; Xiong, Y.; Pramod, K.; Nodari, N. *J. Phys. Chem.* **1992**, *96*, 421. (d) Etter, M. C.; Urbanczyk-Lipkowska, Z.; Ziaebrahimi, M.; Panunto, T. W. *J. Am. Chem. Soc.* **1990**, *112*, 8415.
(13) Heine, H.-G.; Hartmann, W.; Kory, D. R.; Magyar, J. C.; Hoyle, C. E.; McVey, J. K.; Lewis, F. D. *J. Org. Chem.* **1974**, *39*, 691.
(14) McKenzie, A.; Rogers, R.; Wills, G. O. *J. Chem. Soc.* **1926**, 778.

Table 1. Details of Data Collection and Structure Refinement for 1,2-Diphenyl-2-methyl-1-propanone

formula	$C_{16}H_{16}O$
fw	224.30
cryst syst	monoclinic
space group	$P2_1/n$
cryst dimens, mm	0.35 × 0.42 × 0.25
cryst color	colorless
cryst habit	irregular
a, Å	17.916(1)
b, Å	6.380(1)
c, Å	11.744(1)
β, deg	103.81(1)
Z	4
V, Å^3	1303.7(2)
ρ(calcd), g cm^{-3}	1.14
radiation, λ	Mo Kα, 0.7107
F(000), e	480
temp, K	298
diffractometer	Huber (Crystal Logic)
scan mode, speed(deg/min)	θ–2θ, 12.0
2θ range, deg	1–50
total data collcd, unique data used	2593, 1203 ($I > 3\sigma(I)$)
no. of parms refined	154
final shift/error, max and avg	0.005, 0.001
max resid density, e/Å^3	0.26
$R = \sum\|\|F_o\| - \|F_c\|\|/\sum\|F_o\|$	0.050
$R_w = (\sum w(\|F_o\| - \|F_c\|)^2/\sum w(\|F_o\|)^2)^{1/2}$	0.062
GOF = $(\sum w(\|F_o\| \|F_c\|)^2/(N_o - N_v))^{1/2}$	1.845

p-di-*tert*-butylbenzene at 31.0 ppm vs TMS was used as a chemical shift reference and for instrumental adjustment. Some spectra were recorded with total spinning sideband suppression.[15] Typically, 100–200 scans with 4K data points zero filled to 8K were acquired after evaluation of the optimum contact times (3.5 ms) and recycle delays (4 s) so that relative signal intensities reasonably reflect spin concentrations. Solid-state IR spectra were recorded in a Nicolet 510P FT instrument in pressed KBr pellets, X-ray powder diffraction patterns were obtained in a locally constructed diffractometer. Details of single-crystal X-ray diffraction data collection and refinement are included in Table 1. A list of fractional coordinates and equivalent isotropic thermal parameters (A^2) is shown in Table 2.

Computational Details. Molecular mechanics calculations were carried out with MacroModel V3.5X and BatchMin V3.5.[16] The MM2[17] and MM3[18] force fields and default settings in MacroModel were used as supplied. The initial geometry of **2** for all energy minimizations came from X-ray coordinates. Initial geometries of **1** were generated by replacing one of the methyl groups in X-ray coordinates of **2** by a hydrogen atom with the appropriate bond length. We used a grid search method (MULTC in MacroModel)[19] to carry out conformational analyses of **1** and **2**. Initial geometries for grid searches came from optimized X-ray coordinates. The three torsional angles involved in grid searches are as follows:

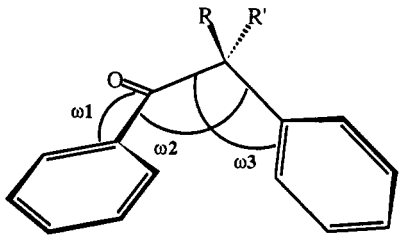

Torsional angles were varied by 60° in each variation. The two lowest-energy conformers located by MM2 were further minimized with AM1[20] or the density functional theory[21] with the local density approximation (program DMOL with DNP basis set with fine mesh). Cavity and cluster minimizations were carried out with the substructure minimization method (SubsM) in MacroModel.

Table 2. Fractional Atomic Coordinates and Equivalent Isotropic Thermal Parameters (Å^2) with esd's of the Refined Parameters in Parentheses for 1,2-Diphenyl-2-methyl-1-propanone[a]

atom	x	y	z	$U_{eq} \times 10^4$
C(1)	0.7492(2)	−0.0903(5)	1.0018(3)	690(25)
C(2)	0.8069(2)	−0.1623(7)	0.9529(4)	992(27)
C(3)	0.8378(2)	−0.0405(10)	0.8815(4)	1117(43)
C(4)	0.8100(2)	0.1578(9)	0.8568(3)	987(36)
C(5)	0.7522(2)	0.2344(5)	0.9060(3)	666(24)
C(6)	0.7209(1)	0.1113(4)	0.9792(2)	470(19)
C(7)	0.6603(2)	0.2029(4)	1.0364(2)	502(20)
C(8)	0.6047(2)	0.3414(5)	0.9490(3)	613(25)
C(9)	0.5530(2)	0.2521(5)	0.8393(2)	516(20)
C(10)	0.4937(2)	0.3798(5)	0.7788(3)	730(27)
C(11)	0.4457(2)	0.3133(7)	0.6759(4)	910(33)
C(12)	0.4559(2)	0.1206(7)	0.6309(3)	913(32)
C(13)	0.5137(2)	−0.0090(6)	0.6896(3)	726(26)
C(14)	0.5622(2)	0.0552(5)	0.7941(3)	573(22)
C(15)	0.6128(2)	0.0371(5)	1.0828(3)	715(25)
C(16)	0.7028(2)	0.3366(5)	1.1401(3)	745(26)
O(1)	0.6010(2)	0.5266(4)	0.9680(3)	1171(26)
H(1A)	0.7257	−0.1838	1.0520	380[b]
H(2A)	0.8274	−0.3073	0.9716	380[b]
H(3A)	0.8809	−0.0967	0.8497	380[b]
H(4A)	0.8326	0.2397	0.8006	380[b]
H(5A)	0.7349	0.3819	0.8865	380[b]
H(10A)	0.4872	0.5239	0.8086	380[b]
H(11A)	0.4002	0.3989	0.6360	380[b]
H(12A)	0.4223	0.0736	0.5545	380[b]
H(13A)	0.5229	−0.1463	0.6541	380[b]
H(14A)	0.6025	−0.0429	0.8378	380[b]
H(15A)	0.5871	−0.0562	1.0167	380[b]
H(15B)	0.5730	0.1063	1.1168	380[b]
H(15C)	0.6478	−0.0483	1.1447	380[b]
H(16A)	0.7356	0.4422	1.1120	380[b]
H(16B)	0.7360	0.2452	1.2009	380[b]
H(16C)	0.6644	0.4107	1.1750	380[b]

[a] $U_{eq} = [1/(6\pi^2)]\sum_i\sum_j\beta_{ij}a_i \cdot a_j$. [b] Denotes isotropic atom (positions and temperature factors not refined).

Results and Discussion

Crystallization and X-ray Analysis. Compound **2** forms large prisms (mp = 45.0–46.0 °C) and crystallizes from several solvents and from the melt in the centrosymmetric space group $P2_1/n$ with one molecule per asymmetric unit. The details of data collection and refinement are contained in Table 1. The molecular structure of **2** (Figure 1) is characterized by C_1 symmetry, and while it is chiral in the solid state, the centrosymmetric space group guarantees the presence of the two enantiomers in the crystal. As in other aryl ketones, there is a nearly coplanar arrangement between the carbonyl group and the phenyl ring which make a dihedral angle of 19.2°. The orientation of the (dimethyl)benzyl substituent involves eclipsing of one of the methyl groups with the carbonyl with a dihedral

(15) Dixon, W. T.; Shaefer, J.; Sefcik, M. D.; McKay, R. A. *J. Magn. Reson.* **1982**, *49*, 341.
(16) Still, W. C. MacroModel V3.5X and BatchMin V3.5, Department of Chemistry, Columbia University, New York, NY 10027.
(17) Allinger's MM2 force field with additional parameters from MacroModel. Key references for MM2: Allinger, N. L. *J. Am. Chem. Soc.* **1977**, *99*, 8127. Burkert, U.; Allinger, N. L. *Molecular Mechanics*; ACS Monograph 177; American Chemical Society: Washington, D.C., 1982.
(18) Allinger's MM3 force field with additional parameters from MacroModel. Key references for MM3: Allinger, N. L.; Yuh, Y. H.; Lii, J.-H. *J. Am. Chem. Soc.* **1989**, *111*, 8551. Allinger, N. L.; Li, F.; Yan, L.; Tai, J. C. *J. Comput. Chem.* **1990**, *11*, 868.
(19) Multic Conformational Search: Lipton, M.; Still, W. C. *J. Comput. Chem.* **1988**, *9*, 343.
(20) Spartan V2–4.0. Wavefunction, Inc., 18401 von Karman Ave., Suite 210, Irvine, CA 92715. Reference for AM1: Dewar, M. J. S.; Zoebisch, E. G.; Healy, E. F.; Stewart, J. J. P. *J. Am. Chem. Soc.* **1985**, *107*, 3902.
(21) DMol V2.2. Biosym Technologies, Inc., 10065 Barnes Canyon Road, San Diego, CA 92121.

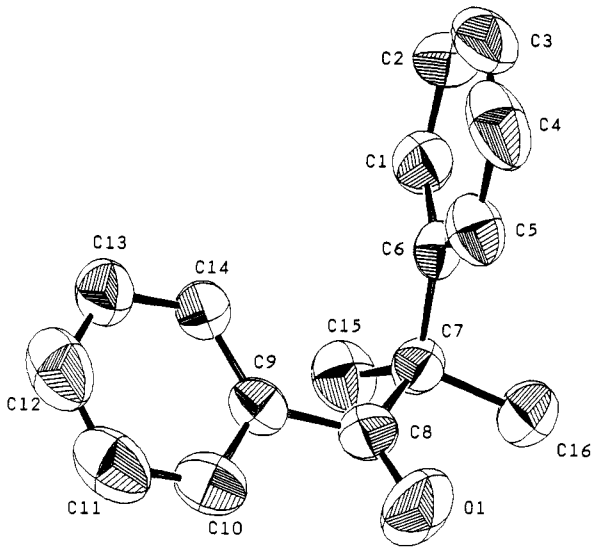

Figure 1. X-ray molecular structure of 1,2-diphenyl-2-methyl-1-propanone (**2**).

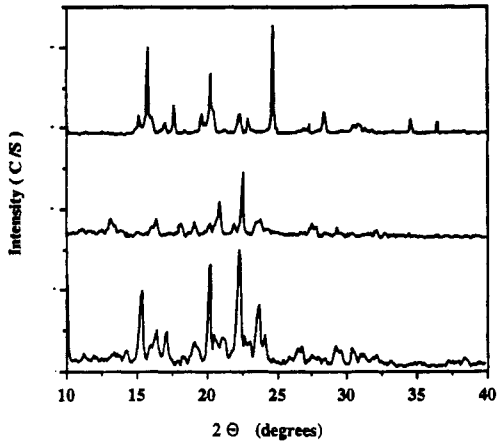

Figure 2. From top to bottom: X-ray powder patterns of 1,2-diphenyl-2-methyl-1-propanone (**2**), (*R,S*)-1,2-diphenyl-1-propane, and (*S*)-(+)-1,2-diphenyl-1-propanone.

angle (O=C—C—Me) of 9.7°. The other methyl group has a dihedral angle (O=C—C—Me) of 126.0°. The α-phenyl group is nearly orthogonal to the plane of the carbonyl (O=C—C—Ph, -107.9°) while the plane of the ring orients with a dihedral angle of 44.4° with the (CO)C-C(Ph) bond.

Samples of (+)-**1** and (±)-**1** form thin needles (mp = 34–35 and 49.5–51.0 °C, respectively) with distinctive solid-state FT-IR and X-ray powder patterns (Figure 2) assigned to the racemic compound and the enantiomorphous phase. Large background and signal broadening in the X-ray powder patterns are indicative of low crystal qualities in the two forms of **1**. They also rule out isomorphism with the structure of **2**. X-ray structural determinations of either form of **1** have not been possible due to the small size and low quality of the crystals and to complications brought by a partial spontaneous resolution in the case of the racemic sample, as detected from ^{13}C CPMAS measurements (vide infra).

Mixed crystals prepared by slow evaporation of solutions containing variable amounts of the two components were obtained with up to ca. 5 ± 1 mol % **1** in crystalline **2**. Solution samples containing larger amounts of **1** failed to crystallize under various conditions including temperatures as low as -30 °C. Experimental information regarding the identity of the mixed crystal phase (0.5–5 mol % **1**) as the same of pure **2** was obtained by X-ray powder diffraction patterns and solid state FT-IR and NMR spectroscopy. Information on the structure of the guest was obtained by high-resolution CPMAS-NMR techniques on samples containing ^{13}C-Me-labeled **1** after the spectra of the pure specimens were analyzed.

Table 3. Solution ($CDCl_3$) and Solid-State (CPMAS) ^{13}C NMR Chemical Shift Data for 1,2-Diphenyl-2-propanone (1) and 1,2-Diphenyl-2-methyl-2-propanone (2)

sample/ signal	**2**, $CDCl_3$ (d)	**2**, CPMAS (d)	**1**, $CDCl_3$ (d)	(±)-**2**, CPMAS (d)	(*S*)-(+)-**2** CPMAS (d)
C=O	204	200.5	200.4	200.1	198.1
Ar	145.3	146.5	141.5	144.8	141.8
	136.3	135.3	136.5	141.3	135.8
	131.7	131.9	132.8	139.7	132.3
	129.7	130.5	129.0	136.5	130.5
	129.0	128.3	128.8	134.5	129.3
	127.9	126.6	128.5	132.9	128.1
	126.8	124.0	127.8	131.1	126.1
	126.7		126.9	129.1	
				126.1	
C (quaternary)	51.4	51.0	47.9	47.9	47.0
Me	27.8	32.5	19.6	21.5	18.2
		22.1			

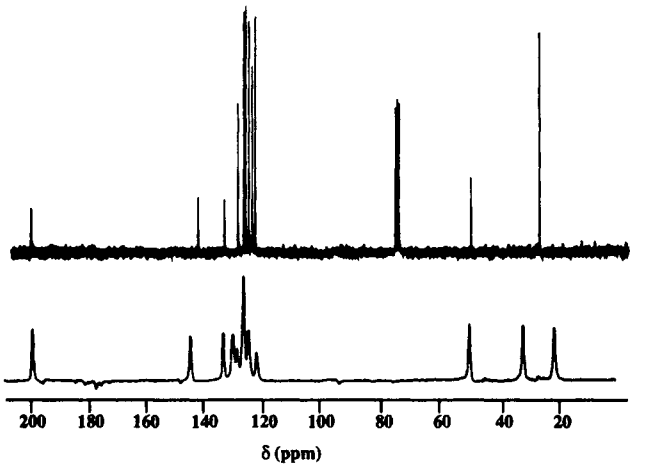

Figure 3. ^{13}C NMR spectra of 1,2-diphenyl-2-methyl-1-propanone in $CDCl_3$ solution (top) and in the solid state (bottom).

Solid-State NMR and Preparation of Mixed Crystals. ^{13}C NMR CPMAS[22] spectra were recorded at 300 MHz with ^1H decoupling fields of ca. 40 kHz at rotor speeds of 4–5 kHz with carefully matched Hartman–Hahn conditions and suitable contact times (3.5 ms) and recycle delays (4 s). The lack of molecular symmetry as revealed by the X-ray analysis is evident in the NMR spectrum with single lines for the C=O, the nonprotonated aromatic carbons, the quaternary aliphatic carbon and the two methyl groups (Table 3). The 10 remaining aromatic carbons appear in a group of five signals between 131.7 and 126.7 ppm. The nonequivalence of the two methyl groups of **2** in the solid state in the ^{13}C CPMAS NMR spectrum with chemical shifts at δ = 22.1 and 32.5 ppm relative to the external *p*-di-*tert*-butyl benzene (Me at 31 ppm vs TMS) is noteworthy (Figure 3). The time-averaged enantiotopic methyl group signals occur at δ = 27.8 ppm in $CDCl_3$ solutions. Racemic samples of ketone **1** crystallized from pentane, ethanol, and the melt gave rise to solid-

(22) (a) Pines, A.; Gibby, M. G.; Waugh, J. S. *J. Chem. Phys.* **1973**, *59*, 569. (b) Fyfe, C. F *Solid State NMR for Chemists*; C.F.C. Press: Guelph, Ontario, 1983.

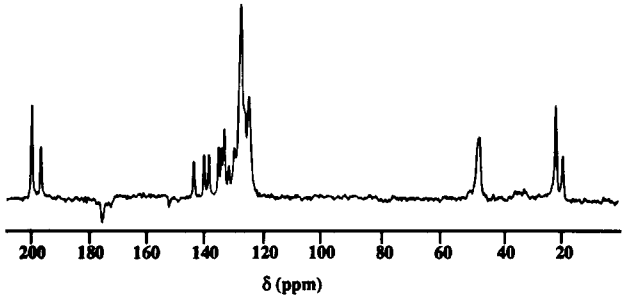

Figure 4. ^{13}C CPMAS NMR spectra of 1,2-diphenyl-2-methyl-1-propanone. Signals corresponding to two crystal phases, assigned to the racemic and the enantiomorphous form, are clearly evident.

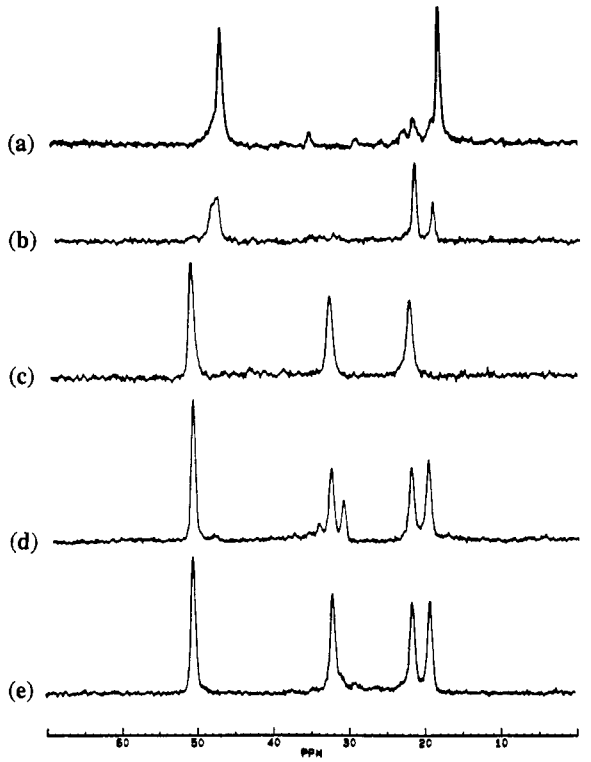

Figure 5. Aliphatic region of the ^{13}C CPMAS NMR spectra of (a) (*S*)-(+)-1,2-diphenyl-1-propane [(**S**)-(+)-1]; (b) (*R,S*)-1,2-diphenyl-1-propane [(**R,S**)-1]; (c) 1,2-diphenyl-2-methyl-1-propanone (**2**); (d) mixed crystals containing with ca. 1.5% mol % (**R,S**)-1; (e) mixed crystal prepared with 1% mol % (**R,S**)-1.

state spectra composed of two sets of peaks with relative intensities of ca. 70 and 30% (Figure 4). These sets of signals correspond to two crystal phases assigned to the racemic compound and to the enantiomorphic phase.[23] This was demonstrated by measuring the spectrum of a sample enriched in the (*S*)-(+)-isomer. Further evidence for these two phases is also available from their X-ray powder patterns. Their chemical shifts and those of compound **2** are included in Table 3.

Solid-state NMR measurements with labeled guest in mixed crystalline samples reflect structural details and information on the host at the molecular level. This is primarily obtained from the sp_3 region of the spectra where the signals corresponding to the ^{13}C-Me labeled guest are expected (Figure 5). For reference purposes, the spectra of 1,2-diphenylpropanone (Figure 5a,b) and 1,2-diphenyl-2-methyl-1-propanone (Figure 5c) were included. Samples

(23) Jacques, J.; Collet, A.; Wilen, S. H. *Enantiomers, Racemates and Resolutions*; John Wiley & Sons: New York, 1981.

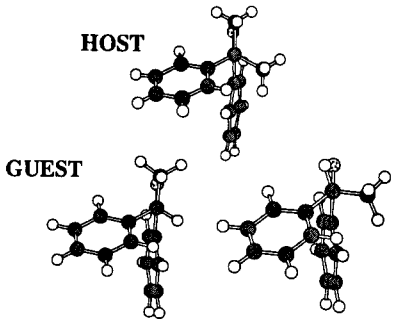

1R-A
Lowest Minimum

1S-B
Second Lowest Minimum

Figure 6. MM2 structures of the dimethyl ketone host and the two lowest energy conformers of the monomethyl ketone guest. The two conformers of **1** are shown as two different enantiomers in the figure to emphasize the overlap with the structure of **2**. The structure of enantiomer **1R** in conformation **B**, for instance, would not have a good overlap with the structure of the **2** represented in the figure. However, **1R-B**, would have a good overlap with the other enantiomer of **2**.

of the monomethyl ketone correspond to crystallizations with optically active and racemic samples, respectively. Also included in the figure are two spectra representative of polycrystalline samples obtained from pentane solution (in ca. 1 h) with 1–2 % of ^{13}C-Me-labeled **1** (≥99%) in dimethyl ketone **2** (Figures 5,e). Signals corresponding to the host can be readily identified by comparison with the spectrum in **Figure 5c** and additional signals in the methyl region of the spectra are assigned to the ^{13}C-labeled guest.

The chemical shift of the ^{13}C-methyl group should be determined by its magnetic environment in the crystal host. To the extent that the structure of the guest mimics the structure of the host, there may be two magnetically different environments that the methyl of the guest may occupy (Figure 6). Crystallization of the guest in a single conformation and orientation is expected to result in a single signal with a solid-state chemical shift similar to that of one of the methyl groups in compound **2**. This is proposed for spectra such as that shown in Figure 5e. In contrast, if mixed crystallization occurs with disorder, one may expect signals of **1** corresponding to the two different replacement alternatives. Chemical shifts of the guest may occur at about 32 and 22 ppm with intensities reflecting their relative contributions. This alternative may be postulated for samples giving rise to spectra such as that in Figure 5d with signals from the guest at 19.0, 31.0, and 34.5 ppm.

Mixed crystallization in both cases occurs under kinetic conditions with multiple nucleation sites and fast crystal growth. The two types of spectra differ only in the region between ca. 30 and 37 ppm (Figures 5d,e). Initially, samples corresponding to Figure 5d were obtained in several runs. Subsequently, up to 15 new samples corresponding to Figure 5e were obtained after a period of 3 months from the initial experiments. Attempts to obtain samples giving rise to spectra such as that in Figure 5d from pentane, ethanol, and hexane solutions of various concentrations and from the melt have been unsuccessful. However, since all the samples were prepared with compounds from the same stock, it is unlikely that impurities should account for the additional peaks in the spectrum of Figure 5d, and we suggest that they correspond to an authentic disordered case.

Chart 3

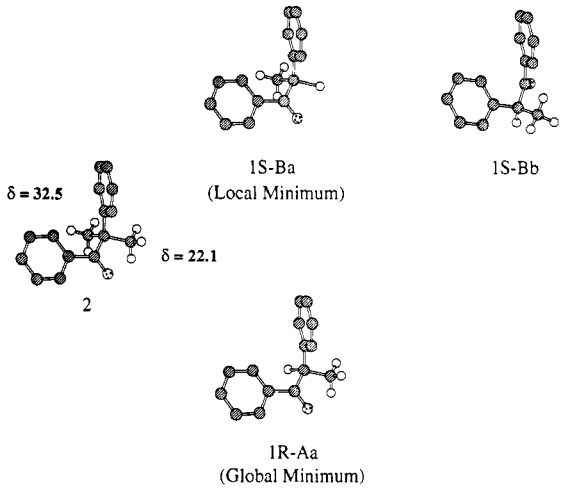

Conformational and Structural Analysis. With the X-ray structure of **2** at hand, the possibilities for mixed crystallization may be analyzed in some detail in order to assign the signals in the NMR spectra and to evaluate the authenticity of the disordered mixed phase. We start by noting that pioneering theories of mixed crystallization proposed by Kitaigorodskii[1] suggest that molecules with a large optimized structural overlap should be capable of forming substitutionally random solid solutions.[1] Quantitatively, the geometric congruence between the two components of a prospective solid solution is obtained in terms of the coefficient of structural similarity, ϵ (eq 1),

$$\epsilon = 1 - [\text{nonoverlapping volume/overlapping volume}] \quad (1)$$

obtained by comparing the overlapping and nonoverlapping volume of the two components. It was postulated that mixed crystallization should be guaranteed in the absence of perturbations to strong packing forces (e.g., hydrogen bonding and ionic interactions) when $\epsilon \geq 0.85$. An ideal situation ($\epsilon_{max} = 1$) would be achieved when the overlap between two components is perfect,[24] while unfavorable size and shape mismatches would give small or negative ϵ values. For compounds **1** and **2**, an $\epsilon \approx 0.92$ value has been estimated with a qualitative volume increment approach.[25]

As suggested in the Introduction and as indicated in Chart 3, a high ϵ may be in principle obtained when **2** is replaced by either of the two enantiomers of **1** (**1R** and **1S**) in two different conformations (**A** and **B**) and possibly in two different orientations, e.g., **a** and **b**. Within limitations of a relatively large overlap while maintaining standard bond lengths and angles, these variations give rise to three different structures for which one may expect different chemical shifts for the ^{13}C-Me probe.

Substitution of **2** with structures such as **1R-Aa** and **1S-Ba** involves the replacement of either methyl group in **2** by a hydrogen in **1** while structures **1S-Bb** involves the exchange of methyl and carbonyl groups. These groups have similar volumes, 22.32 and 18.22 Å^3 for Me and CO, respectively,[25] and may in principle replace each other in the crystal lattice. While it is apparent that structural similarity of the host with the guest may be obtained in various conformers and orientations, it is unlikely that a satisfactory optimized overlap should be sufficient for mixed crystallization without consideration of the conformational energies of the guest. We have therefore carried out a detailed conformational analysis of the guest both in the gas phase and in a model crystal. After evaluating the adequacy of this computational results we have modeled the mixed crystal by replacement of dimethyl ketone **2** by the monomethyl guest **1** in the three structural alternatives of Chart 3.

Modeling of the Pure Crystal Host. The X-ray structure of dimethyl ketone **2** features a methyl group eclipsed to the carbonyl group. The other two substituents, a methyl and a phenyl group, occur gauche to the phenyl group attached to the carbonyl. This preference for alkyl groups to adopt conformations eclipsed with a carbonyl has been found by experiments and theory for many simple ketones and aldehydes.[26,27] This conformation is stabilized by favorable electrostatic (or dipole-induced dipole) interactions between methyl and carbonyl groups[26,27] and by the absence of a group eclipsed to the phenyl group in **2**. Both MM2 and MM3 predict this conformation for the global minimum. The second lowest-energy conformation is 3.3 and 5.8 kcal/mol higher than the global minimum according to MM2 and MM3, respectively.

To test the effect of neighboring molecules on the structure **2**, we carried out minimizations with molecular clusters of different sizes built with the X-ray coordinates. These were carried out at two stages that we called "cavity" and "cluster" minimizations. In the "cavity" minimization, only the central molecule was involved in geometry optimizations while 20 surrounding molecules were held at their X-ray coordinates. Energy terms involving these fixed molecules were included in the total energy evaluation (Figure 7). To allow for partial relaxation, "cluster" minimizations were carried out, in which a cluster of 16 closest neighboring molecules[28] was fully optimized, while additional atoms within 5 Å of the cluster molecules were held fixed but included in the energy evaluation. Using this 5 Å criterion, up to 1007 atoms belonging to fragments of 54 surrounding molecules were included in the cluster energy calculations.

The results from cavity and cluster minimizations for the central molecule in crystal of **2** are listed in Table 4. For comparison reasons, a monomer of **2** was minimized in the gas phase also starting from its X-ray coordinates. As can be seen in Table 4, the gas-phase results are lowest in energy but deviate the most from the X-ray coordinates. For example, when MM2 was used, the root-mean-squared (rms) deviations of the central molecule from the X-ray geometry were 0.174, 0.155, and 0.123 Å from the gas phase,

(24) Nearly ideal solid solutions may be expected when mixed crystallization involves simple isotopic substitution: (a) Colson, S. D.; Robinson, G. W. *J. Chem. Phys.* **1968**, *48*, 2550. (b) Klafter, J.; Jortner, J. *Chem. Phys. Lett.* **1977**, *49*, 410. (c) Nieman, G. C.; Robinson, G. W. *J. Chem. Phys.* **1962**, *38*, 2150.

(25) Gavezzotti, A., *J. Am. Chem. Soc.* **1983**, *105*, 5220.

(26) (a) Pickett, H. B.; Scroggin, D. G. *J. Chem. Phys.* **1974**, *61*, 3954. (b) Durig, J. R.; Compton, D. A. C; McArver, A. Q. *J. Chem. Phys.* **1980**, *73*, 719. (c) Abe, M.; Kuchitsu, K.; Shimanouchi, T. *J. Mol. Struct.* **1969**, *4*, 245. (d) Sakurai, T.; Ishiyama, M.; Takeuchi, H.; Takeshita, K.; Fukushi, K.; Konaka, S. *J. Mol. Struct.* **1989**, *213*, 245. (e) Guirgis, G. A.; Little, T. S.; Badawi, H. M.; Durig, J. R. *J. Mol. Struct.* **1986**, *142*, 93.

(27) (a) Wiberg, K. B.; Martin, E. *J. Am. Chem. Soc.* **1985**, *107*, 5035. (b) Wiberg, K. B. *J. Am. Chem. Soc.* **1986**, *108*, 5817. (c) Wiberg, K. B.; Murcko, M. A. *J. Comput. Chem.* **1988**, *9*, 488. (d) Bowen, J. P.; Pathiaseril, A.; Profeta, S., Jr.; Allinger, N. L. *J. Am. Chem. Soc.* **1987**, *52*, 5162. (e) Siam, K.; Van Alsenoy, C.; Klimkowski, V. J.; Ewband, J. D.; Schäfer, L. *J. Mol. Struct. (THEOCHEM)* **1984**, *110*, 327.

(28) Any molecule within 6 Å of an arbitrarily defined central molecule is included in the cluster. As a result, the cluster contains a central molecule which is surrounded by 16 neighboring molecules.

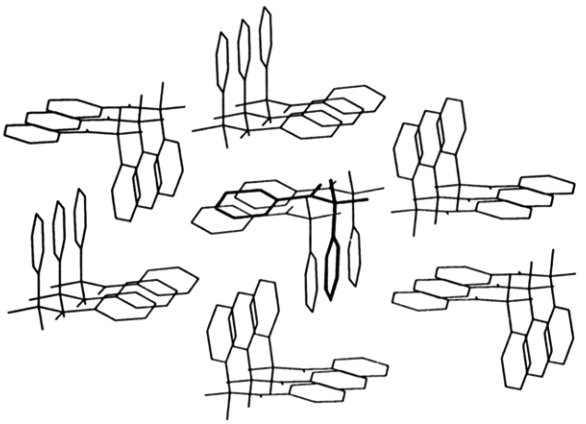

Figure 7. View of the cluster employed for "cavity" MM2 and MM3 minimizations. The reference molecule, dimethyl ketone **2**, sits at the center of the cluster with 20 closest neighbors held at their X-ray coordinates. The minimized cavity structure does not differ from the gas-phase structure or the structure obtained in "cluster minimizations" where the lattice is allowed to minimize. The view shown is close to the direction of translation down the *b* axis.

Table 4. Steric Energies (SE) of Dimethyl Ketone 2 and Root-Mean-Square Deviations between Calculated Positions and That Observed in the X-ray Structure[a]

force field	gas phase SE, kcal/mol (rms, Å)	cavity SE, kcal/mol (rms, Å)	cluster SE, kcal/mol (rms, Å)
MM2	15.49 (0.174)	15.61 (0.155)	15.63 (0.123)
MM3	23.05 (0.207)	23.38 (0.123)	23.36 (0.107)

[a] Minimization was carried out with and without surrounding molecules using MM2 and MM3 force fields in MacroModel. For cavity and cluster minimizations, only values of the central molecule were reported.

cavity, and cluster minimizations, respectively. MM3 results showed the same decreasing trend in rms values when the size of calculated systems increased. It is encouraging that the calculated geometry of **2** is closer to the X-ray geometry when the models are closer to the real crystal. These calculations suggest that packing interactions raise the energies of individual molecules in the crystal only by a small amount. According to MM2 and MM3, the energy of the central molecule increases by 0.1 and 0.3 kcal/mol, respectively, when surrounded by other molecules. This is more than compensated for by stabilizing intermolecular interactions.

Modeling the Mixed Crystal. The effect of including a guest molecule such as **1** in crystals of **2**, was carried out by cavity and cluster minimizations with a reference molecule of dimethyl ketone **2** at the center of the ensemble replaced by monomethyl ketone **1**. We refer to these as replacement calculations.

Conformational analyses of **1** with MM2 and MM3 both showed that the two lowest energy conformations, **1-A** and **1-B**, were good candidates for replacing a molecule of **2** in crystal so long as two enantiomers (e.g., **1R-A** and **1S-B** in Chart 3) are utilized for replacement of the two enantiotopic methyl groups. It should be stressed that the crystal is centrosymmetric, and reflection of Chart 3 in a mirror describes substitution at enantiomerically related sites of **2**. Conformers **1-A** have a methyl group eclipsed with the carbonyl group while this position is taken by a hydrogen in **1-B**, the second lowest conformation (Figure 7). Energy differences between **1-A** and **1-B** were 2.6, 3.2, 1.7, and 2.3 kcal/mol according to MM2, MM3, AM1, and local density functional (LDF) calculations, respectively. Previous studies of propanal, 2-butanone, isobutyraldehyde, and methyl isopropyl ketone showed energy differences of 1–2 kcal/mol between these two kinds of conformers.[29,30] Since the MM2 energy difference of **1-A** and **1-B** (2.6 kcal/mol) was closer to the LDF results (2.3 kcal/mol), we based our discussion on the MM2 results. However, trends in MM3 results were still examined and compared to those from MM2 results.

Table 5. Results of Cavity Minimizations with a Reference Molecule Replaced with 1R-Aa, 1S-Ba, or 1S-Bb (See Chart 3)

	MM2		MM3	
system	SE_{total} [$SE_{central}$], kcal/mol	DSE_{total} [$DSE_{central}$], kcal/mol	SE_{total} [$SE_{central}$], kcal/mol	DSE_{total} [$DSE_{central}$], kcal/mol
1R-Aa[a]	454.57 [10.57]	0.00 [0.00]	623.69 [19.00]	0.00 [0.00]
1S-Ba[b]	457.39 [13.18]	2.82 [2.61]	627.48 [22.36]	3.79 [3.36]
1S-Bb[b]	461.61 [14.86]	7.04 [4.29]	632.01 [24.04]	8.32 [5.04]

[a] Gas-phase steric energy of **1-A** is 10.30 kcal/mol by MM2 and 18.54 kcal/mol by MM3. [b] Gas-phase steric energy of **1-B** is 12.94 kcal/mol by MM2 and 21.72 kcal/mol by MM3.

Conformation **1-B** has a quasi-C_2 axis (Scheme 5), and it is conceivable that **1-B** might be included in crystal lattice in orientations designed with the labels **a** and **b** as in **1S-B*a*** and **1S-B*b*** in Chart 3:

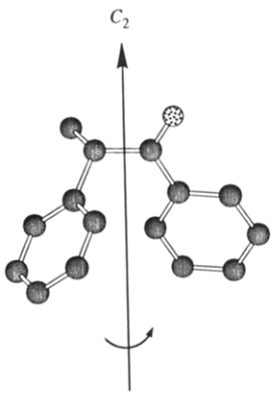

A similar replacement for the lowest energy conformer **1R-Aa** (e.g., **1R-Ab**, not shown above) would result in a very large structural mismatch with the structure of the host **2** unless severe geometrical distortions are imposed at the benzoyl group. This replacement was not considered in our calculations. A total of three sets of displacement calculations was carried out. Following the nomenclature of Chart 3, these were termed **1R-Aa** and **1S-Ba**, when either methyl group in **2** is replaced by the methyl group of **1**, and **1S-Bb**, when replacement of the carbonyl by a methyl groups is considered.

The results from replacement calculations are summarized in Tables 5 and 6. As observed for the central molecule in a pure crystal of **2**, energies of **1a** and **1b** were also raised slightly upon crystal packing. For example, the MM2 energies of **1a** in cavity and cluster minimizations are 10.57 and 10.61 kcal/mol, respectively, which are 0.3 kcal/mol higher than the corresponding gas-phase minimum.

(29) Bovey, F. A.; Jelinski, L.; Mirau, P. A., *Nuclear Magnetic Resonance Spectroscopy*; Academic Press: New York, 1992; Chapter 3.
(30) Ferguson, L. N. *Organic Molecular Structure*: Willard Grant; Boston, 1975; p 134.

Table 6. Results of Cluster Minimizations with Reference Molecule Replaced with 1R-Aa, 1S-Ba, and 1S-Bb (See Chart 3)

	MM2		MM3	
system	SE_{total} [$SE_{central}$], kcal/mol	DSE_{total} [$DSE_{central}$], kcal/mol	SE_{total} [$SE_{central}$], kcal/mol	DSE_{total} [$DSE_{central}$], kcal/mol
1R-Aa[a]	155.24 [10.61]	0.00 [0.00]	364.79 [19.02]	0.00 [0.00]
1S-Ba[b]	158.10 [13.25]	2.86 [2.64]	368.72 [22.35]	3.93 [3.33]
1S-Bb[b]	162.03 [14.47]	6.79 [3.86]	372.36 [23.71]	7.57 [4.69]

[a] Gas-phase steric energy of **1-A** is 10.30 kcal/mol by MM2 and 19.54 kcal/mol by MM3. [b] Gas-phase steric energy of **1-B** is 12.94 kcal/mol by MM2 and 21.72 kcal/mol by MM3.

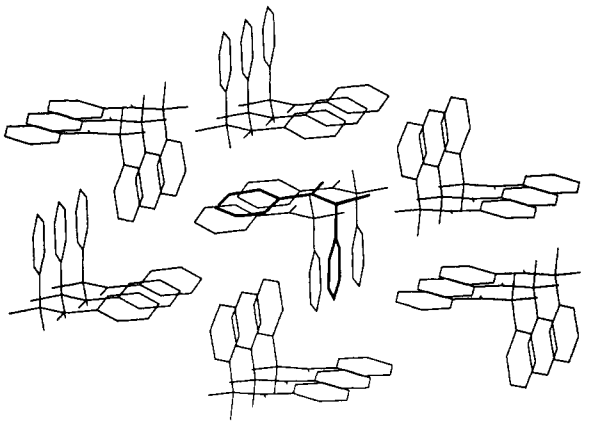

Figure 8. View of the MM2 minimized "cavity" of monomethyl ketone **1** with structure **1R-Aa** (global energy minimum with Me by H replacement). The reference molecule, sits at the center of the cluster with 20 close neighbors. Very small conformational and packing distortions are observed. The view is close to the direction of translation down the *b* axis.

Both cavity and cluster calculations showed **1R-Aa** is the best candidate for inclusion in crystal of **2** (Figure 8). Use of **1S-Ba**, the second lowest energy conformer (not shown), increased the system energy by ca. 2.8 kcal/mol (DSE_{total} in Tables 5 and 6). Interestingly, 93% of this energy difference came from the energy difference between **1R-Aa** and **1S-Ba** in the crystal ($DSE_{central}$), which was ca. 2.6 kcal/mol. *We take this result as an indication that the crystal host may bind guests **1R-Aa** and **1S-Ba** nearly equally well. Crystal packing interactions do not exacerbate the gas phase energy differences.* Furthermore, the fact that results from cavity and cluster calculations are very similar shows that **1R-Aa** and **1S-Ba** may both fit snugly in the crystal lattice. For example, the $SE_{central}$ of **1R-Aa** in the cavity minimization differed from that in the cluster minimization by only 0.04 kcal/mol.

When **1S-Bb** was put into the central position with the second orientation suggested by the quasi-C_2 axis, the energies from cavity minimization of the system (SE_{total}) and the guest ($SE_{central}$) were 4.2 and 1.7 kcal/mol higher, respectively, than that in the alternative orientation (**1S-Ba**). It should also be pointed out that $DSE_{central}$ was no longer a major component of DSE_{total} and that a large perturbation of the crystal was taking place (Figure 9). In addition, values of $SE_{central}$, DSE_{total}, and $DSE_{central}$ for **1S-Bb** in the more flexible cluster minimization were 0.3–0.4 kcal/mol smaller than that from the cavity minimization. Therefore, when **1S** was included in a crystal of **2** in orientation **1S-Bb**, both **1S** and the surrounding molecules were forced to distort from their ideal positions or conformations. Cluster minimization reduced the strain in the system; the energy decrease was small (0.3–0.4 kcal/mol). Inclusion of more molecules than those already present in current cluster calculations is unlikely to have a significant effect.

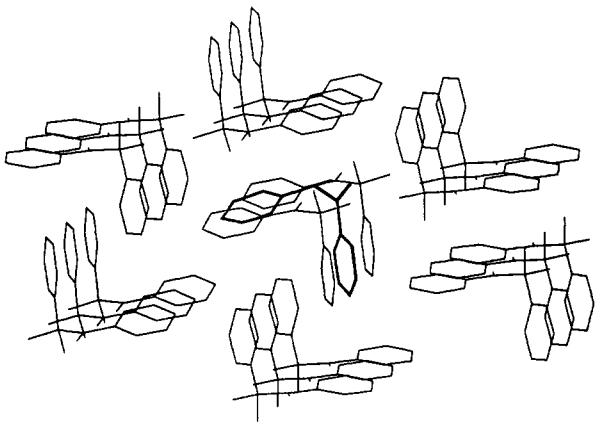

Figure 9. View of the MM2 minimized "cavity" of monomethyl ketone **1** with structure **1S-Bb** , the second lowest energy minimum of **1** with a methyl group of **1** occupying the position of the carbonyl group of **2**. The reference molecule sits at the center of the cluster with 20 close neighbors. Large conformational distortions are observed in minimizations where the lattice is held rigid. In contrast, large packing reorganizations are observed when the lattice is allowed to minimize. The view is close to the direction of translation down the *b* axis.

Correlation of NMR and Modeling Studies. The assignments of the two methyl signals of crystalline **2** in the solid state is relevant to the structural characterization of the guest in the mixed crystalline specimens. Solid-state chemical shifts differ from that in $CDCl_3$ solution by deshielding of one of the signals by 4.7 ppm while the other suffers a shielding of 5.7 ppm for a total splitting of 10.4 ppm relative to the solution signal at 27.8 ppm. The molecular disymmetry of **2** in the solid state suggests that this splitting is related to the well-documented splitting of geminal diastereotopic groups in the NMR of liquids.[29] However, the magnitude of the solid-state splitting is unparalleled in solution and originates in the rigidity of the solid state molecular structure. Part of this splitting may originate from the locally anisotropic diamagnetic shielding of the carbonyl and phenyl groups but its magnitude seems to be nearly outside the expected range.[30] It is also possible that anisotropic paramagnetic contributions involving the excited states of the aryl ketone chromophore may be partially responsible for the large chemical shift difference.[31] The signal at 22.1 ppm is tentatively assigned to the methyl group nearly eclipsed to the carbonyl group in analogy with the spectra of monomethyl compound **1**, where the methyl group resonates at 21.5 or 18.2 depending on the crystal phase. This assignment is based on the assumption that the chemical shift of this group is similar to that of **1**, as calculations [MM2, MM3, AM1 and local density functional method (LDF)] predict a very close steric relationship in its lowest energy conformer.[32,33]

(31) Mehring, M. *High Resolution NMR Spectrosocopy in Solids*; Springer-Verlag: Berlin, 1976; Chapter 5.

(32) This assumption is based on the premise that the crystal conformation will be the same as the lowest gas-phase conformer in the absence of strong packing perturbations, which is the case of dimethyl ketone **2** for which the X-ray structure was satisfactorily reproduced by conformational calculations.

(33) Dunitz, J. D. *X-ray Analysis and the Structure of Organic Molecules*; Cornell University Press: Ithaca, NY, 1979.

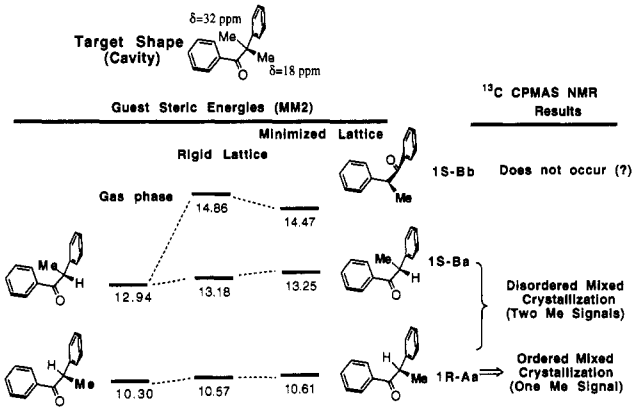

Figure 10. Schematic representation of the correlation between the MM2 conformational energies the guest and the NMR results.

Results of MM2 modeling of the mixed crystal are summarized and presented in Figure 10. The MM3 results show the same trends observed in MM2 results and suggest that the lowest energy conformer of 1 (**1R-Aa**) should be the most suitable structure for mixed crystallization. We propose that samples giving rise to spectra displaying a single resonance at 18 ppm represent the exclusive incorporation of **1R-Aa**. In contrast, samples giving rise to spectra with up to three different signals (**Figure 5d**) indicate simultaneous cocrystallization of different guest structures. A signal at 18 ppm is assigned to **1R-Aa** while signals at 31 and 34.5 ppm correlate with the methyl group anti to the carbonyl group which in the spectrum of the host appears at 32.5 ppm. The latter assignment corresponds to mixed crystallization with structure **1S-Ba** and we speculate that the presence of two signals may imply two closely related but non-identical structures.

The most striking observation from the computational result is that the energetic disadvantage of a non lowest energy conformer, e.g., **1S-Ba,** is not exacerbated by intermolecular interactions in the crystal lattice. It appears that simultaneous substitution of the guest with structures **1R-Aa** and **1S-Ba** would seem likely and give rise to spectra such as that in **Figure 4c**. The entropy of the system should favor incorporation of the guest in more than one conformation and/or orientation. Our computational and experimental results suggests that **1R-Aa** and **1S-Ba** are close in energy and that changes between ordered and disordered mixed crystallization are posed by very subtle and yet to be determined experimental differences. However, it appears that the crystal host may still be quite shape selective. Packing of 1 in the rotated structure **1S-Bb** results in a significant energy increase of both the molecule and its surroundings.

Random Mixed Crystallization and Sectoring. One may hypothesize that the two different mixed crystal forms arise from two different crystal structures of the host where the solute presents differences in solubility. However, this is not supported by our spectral results where no changes are observed when the guest is incorporated to ca. 1–5% levels. Another explanation comes from the possibility that these two types of samples may originate from crystallization conditions differing in terms of kinetic or thermodynamic growth in spite of our inability to detect experimental differences. It has been recently shown that, in contrast to Kitaigordskii's early hypothesis, mixed crystallization under conditions of kinetic growth may occur in a nonstatistical manner.[6] It has been shown that these complications may arise by molecular recognition

Chart 4

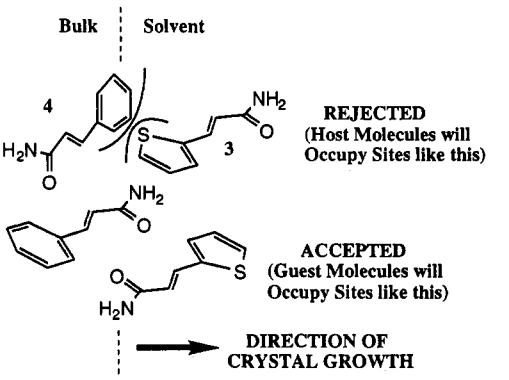

occurring at different faces during crystal growth and that nonrandom substitution results in crystal sectoring and symmetry lowering.[4-6] Since it is possible that sectoring may be the responsible influence for the two types of samples obtained, we now analyze this possibility in some detail.

In one of several well-studied examples by Vaida *et al.*,[6] it was elegantly demonstrated that deposition of 7.5–8% 2-thienylacrylamide (3) occurs along preferred orientations in the growing crystal faces of crystals of cinnamamide 4 (Chart 4). It was shown that a guest molecule accommodating in a prospective crystal site would prefer to position its sulfur atom towards the solvent interface rather than exposing it to the face of a phenyl ring of a host molecule already at the surface. This arrangement should avoid adverse sulfur-to-π-system electronic repulsions. Interestingly, these preferences effectively change the space group of different crystal sectors. Changes in space group were unambiguously determined by detection of "forbidden" X-ray reflections with the help of the "heavy" sulfur atom in the guest, that would not be observed for the pure crystal host. The space group $P2_1/c$ reduces to $P1$ and Pc in different sectors of the mixed crystals with the consequent changes in their systematic absences.

As in the case of 3 and 4, molecular recognition at surface sites during crystal growth of 1 and 2 may result in the macroscopic orientation of the guest molecules relative to defined directions in the crystal host. Since various posible guest orientations are related by the symmetry of the ideal crystal host, CPMAS NMR is insensitive to the possibility of sectoring due to preferential guest orientation. In contrast, dipolar-decoupled single crystal NMR experiments may be valuable in detecting orientational distributions different from those expected from the symmetry of the space group of the host.[34] The relative orientation of the chemical shift tensors of the guest may be tracked relative to the orientation of the external magnetic field. However, because of their rapid rotational reorientation, methyl groups have a very reduced chemical shift anisotropy (CSA) and their use for such experiments should not be as advantageous as with groups with a large CSA such as carbonyl group and others.[34]

Macroscopic Segregation. We have searched for evidence of segregation of the guest in different crystal sectors. Analysis of several fragments of cut single crystals and samples taken from polycrystalline specimens suggest that the distribution of the guest is homogeneous in a given batch. Recognition at different crystal faces may originate from energetic preferences based on hydrogen

(34) Veeman, W. S. *Prog. NMR Spectrosc.* **1984**, *16*, 193.

bonding, electronic repulsion, dipolar interactions and steric effects, but in the case of **1** and **2**, it is likely that only steric effects will be important. One may speculate that a nonrandom crystallization of **1** in crystals of **2** may be based on steric choices given to **1** when approaching the crystal faces with the methyl group towards the interface or away from it. This selection would be likely to have an impact in the direction of growth parallel to the crystallographic *b* axis, resulting in enantiomorphous sectors at opposite directions of crystal growth. An attempt was made therefore to determine whether an enantiomorphic recognition of the guest could have occurred at different sectors. Unfortunately, attempts to carry out solution NMR with a chiral shift reagent could not be utilized to identify an enantiomeric separation of simulated samples when racemic **1** was analyzed in the presence of 99% **2**. An alternative resort based on the use of anomalous birefringence[5] was not attempted.

Conclusions

We have shown that a magnetic label and high-resolution solid-state ^{13}C CPMAS NMR experiments give information on the structure of dilute mixed crystalline samples at the molecular level. Experimental measurements show the formation of two types of mixed crystalline specimens differing in the number of signals assigned to the ^{13}C-labeled guest. To understand the structure of these crystals, we have implemented computational measurements with readily available programs based on current force-field methods. Computational results indicate that the two lowest energy conformers of the guest have relatively small energetic differences and that both have an excellent structural overlap with the host. The results are consistent with a model where mixed crystallization occurs either in an ordered fashion, with host molecules replaced by a unique structure of the guest, or, in a disordered fashion, where the two lowest energy conformers of the guest substitute a host molecule. Further work will be required to distinguishing the factors that control the formation of mixed crystalline phases.

Acknowledgment. We are grateful to the donors of the Petroleum Research Fund, administered by the American Chemical Society, the National Science Foundation, and the College of Letters and Science of the University of California, Los Angeles, for support of this work. We also thank Ms. Yu Hsiou for generating atomic coordinates for lattice calculations.

Supplementary Material Available: Tables containing interatomic distances and bond angles (Table AI) (Table AII) and a listing of the anisotropic temperature factors (Table AIII) from crystals of 1,2-diphenyl-2-methylpropanone (2 pages); listing of the observed and calculated structure factors. Ordering information is given on any current masthead page.